Exceptional service in the national interest

Sandia National Laboratories

SAND2019-3919PE

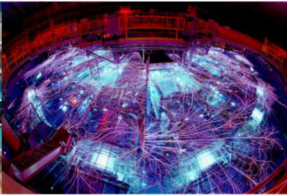

On AFC algorithms for continuous Galerkin discretization of MHD equations

S. Mabuza, J.N. Shadid, S. Conde, E.C. Cyr, T.M. Smith, R.P. Pawlowski
(CCR,Sandia National Laboratories) and D. Kuzmin (TU Dortmund University)

FEF, 2 April 2019

oratories is a multimission laboratory managed and operated by National Technology & Engineering Solutions of Sandia,
neywell International Inc., for the U.S. Department of Energy's National Nuclear Security Administration under contract

Acknowledgments

This material is based upon work supported by the U.S. Department of Energy, Office of Science, Office of Advanced Scientific Computing Research.

Outline

- **Motivation**
- **Introduction**
  - Ideal inviscid MHD model
  - Inviscid Euler equations
  - Hyperbolic systems
- **Numerical method**
  - CG schemes for hyperbolic systems
  - Stabilized schemes for hyperbolic systems
- **Numerical studies**
  - 1D MHD test
  - 2D MHD test

Motivation

Solution to strongly coupled multiphysics problems, often involving strong shocks:

1) be positivity preserving for ρ, internal energy etc. (e.g. LED schemes),
2) be applicable to widely varying timescales,
2.1) allow flexible time integrator usage (e.g. RK-IMEX schemes),
3) be on general unstructured meshes, high spatial and temporal order,
4) hyperbolic system solver applied to the multi-fluid plasma model.

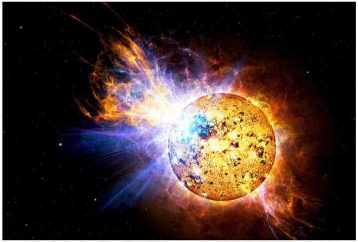

Astrophysical plasma (Casey Reed/NASA)

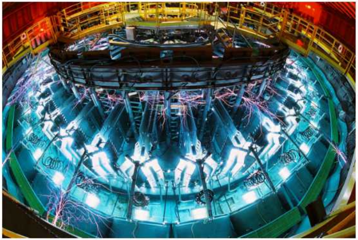

Laboratory plasma (SNL)

Ideal compressible MHD equations

The inviscid MHD equations are given by:

$$\frac{\partial}{\partial t}\begin{bmatrix}\rho \\ \rho \boldsymbol{v} \\ \rho E \\ \boldsymbol{B}\end{bmatrix} + \nabla \cdot \begin{bmatrix}\rho \boldsymbol{v} \\ \rho \boldsymbol{v} \otimes \boldsymbol{v} + p I - \boldsymbol{T}_M \\ \boldsymbol{v} \cdot ((\rho E + p) I - \boldsymbol{T}_M) \\ \boldsymbol{B} \otimes \boldsymbol{v} - \boldsymbol{v} \otimes \boldsymbol{B}\end{bmatrix} = \boldsymbol{0}.$$

Divergence free involution:

$$\nabla \cdot \boldsymbol{B} = 0.$$

ρ is the density. $\boldsymbol{v}$ is fluid velocity. $\rho \boldsymbol{v}$ is fluid momentum. ρE is the total energy. $\boldsymbol{B}$ is the magnetic field. μ_0 is the fluid permeability. γ is the ratio of specific heats.	Total energy: $\rho E = \rho e + \frac{1}{2}\rho \lVert \boldsymbol{v} \rVert^2 + \frac{1}{2\mu_0}\lVert \boldsymbol{B} \rVert^2.$ Ideal equation of state (EOS): $\rho e = \frac{p}{\gamma - 1}, \ \gamma > 0.$ Maxwell stress tensor: $\boldsymbol{T}_M = \frac{1}{\mu_0}\left[\boldsymbol{B} \otimes \boldsymbol{B} - \frac{1}{2}\lVert \boldsymbol{B} \rVert^2 I\right].$

Compressible Euler equations

In the absence of the magnetic field $\boldsymbol{B}$

$$\frac{\partial}{\partial t}\begin{bmatrix}\rho\\ \rho\boldsymbol{v}\\ \rho E\\ \boldsymbol{B}\end{bmatrix}+\nabla\cdot\begin{bmatrix}\rho\boldsymbol{v}\\ \rho\boldsymbol{v}\otimes\boldsymbol{v}+pI-\boldsymbol{T}_M\\ \boldsymbol{v}\cdot((\rho E+p)I-\boldsymbol{T}_M)\\ \boldsymbol{B}\otimes\boldsymbol{v}-\boldsymbol{v}\otimes\boldsymbol{B}\end{bmatrix}=\boldsymbol{0}.$$

$$\rho E=\rho e+\frac{1}{2}\rho\|\boldsymbol{v}\|^2+\frac{1}{2\mu_0}\|\boldsymbol{B}\|^2,\ \rho e=\frac{p}{\gamma-1},\ \gamma>0.$$

we have the compressible Euler equations:

$$\frac{\partial}{\partial t}\begin{bmatrix}\rho\\ \rho\boldsymbol{v}\\ \rho E\end{bmatrix}+\nabla\cdot\begin{bmatrix}\rho\boldsymbol{v}\\ \rho\boldsymbol{v}\otimes\boldsymbol{v}+pI\\ \boldsymbol{v}\cdot((\rho E+p)I)\end{bmatrix}=\boldsymbol{0}.$$

$$\rho E=\rho e+\frac{1}{2}\rho\|\boldsymbol{v}\|^2,\ \rho e=\frac{p}{\gamma-1},\ \gamma>0.$$

Solution strategy:

- Do continuous finite element discretization in space (P^1/Q^1).
- Introduce algebraic stabilization (low order diffusion + limiters).
- Do divergence cleaning for MHD (hyperbolic/parabolic/mixed).

Nonlinear hyperbolic system in a domain $\Omega \subset \mathbb{R}^d$:

$$\mathbf{u}_t + \nabla \cdot \mathbf{f}(\mathbf{u}) = \mathbf{0},\ (\boldsymbol{x}, t) \in \Omega \times \mathbb{R}_+$$
$$\mathbf{u}(\boldsymbol{x}, 0) = \mathbf{u}_0(\boldsymbol{x}),\ \boldsymbol{x} \in \Omega,$$

with suitable boundary conditions.

- $\mathbf{u} : \mathbb{R}^d \times \mathbb{R}_+ \to \mathbb{R}^m$ are the conserved variables.
- $\mathbf{u}_0$ is a given function defining the initial condition.
- $\mathbf{f} : \mathbb{R}^m \to (\mathbb{R}^m)^d$ is the physical flux which is of the form

$$\mathbf{f} = \{\mathbf{f}_i\}_{i=1}^d,\ \mathbf{f}_i \in \mathbb{R}^m,\ i = 1, ..., d.$$

- $\mathbf{f}'(\mathbf{u})$ the Jacobian of the physical flux.

The eigen-decomposition of $\mathbf{f}'$ is:

$$\boldsymbol{n} \cdot \mathbf{f}'(\mathbf{u}) = R(\mathbf{u}; \boldsymbol{n})\Lambda(\mathbf{u}; \boldsymbol{n})R^{-1}(\mathbf{u}; \boldsymbol{n}),$$

where $\boldsymbol{n}$ is a unit vector in $\mathbb{R}^d$, R is the matrix of eigenvectors and Λ is the diagonal matrix of eigenvalues.

Examples of hyperbolic systems include:

- Scalar convection of a chemical in an in/compressible fluid:
  $\mathbf{u} = c$, the concentration, and $\mathbf{f} = \boldsymbol{v}c$, where $\boldsymbol{v}$ is the fluid velocity.
- Scalar Burgers equation (has many applications):
  $\mathbf{u} = u$, the conserved quantity, and $\mathbf{f} = \frac{1}{2}u^2$ the flux.
- Compressible Euler equations:
  $$\mathbf{u} = \begin{bmatrix} \rho \\ \rho \boldsymbol{v} \\ \rho E \end{bmatrix}, \text{ the conserved variables, } \mathbf{f}(\mathbf{u}) = \begin{bmatrix} \rho \boldsymbol{v} \\ \rho \boldsymbol{v} \otimes \boldsymbol{v} + pI \\ \rho E \boldsymbol{v} + p \boldsymbol{v} \end{bmatrix} \text{ the flux.}$$
- Compressible inviscid MHD equations:
  $$\mathbf{u} = \begin{bmatrix} \rho \\ \rho \boldsymbol{v} \\ \rho E \\ \boldsymbol{B} \end{bmatrix}, \text{ the conserved variables, } \mathbf{f}(\mathbf{u}) = \begin{bmatrix} \rho \boldsymbol{v} \\ \rho \boldsymbol{v} \otimes \boldsymbol{v} + pI - \boldsymbol{T}_M \\ \boldsymbol{v} \cdot ((\rho E + p) I_{d \times d} - \boldsymbol{T}_M) \\ \boldsymbol{v} \otimes \boldsymbol{B} - \boldsymbol{B} \otimes \boldsymbol{v} \end{bmatrix} \text{ the flux.}$$

Other examples include shallow water equations, two-fluid plasma equations etc...

The design of numerical methods for hyperbolic systems seeks to achieve the following:

Elimination of spurious oscillations that may result in non-physical solutions (e.g. negative density concentration, internal energy).

Involves:

- Adding sufficient diffusion in the region near a steep front or shock.
- Reduce diffusion in regions with smooth solution (high-resolution).
- Eliminate diffusion completely for linear solutions (linearity-preservation).

Numerical method:

- Should be second order for smooth solutions.
- Work on unstructured meshes.
- Works well with implicit time integration.

The *stabilized* scheme here is based on algebraic flux correction:

- Adding artificial diffusion element-wise.
- Lumping mass matrix associated with the time derivative.
- Controlling the amount of diffusion through a nodal variation based limiter.

Numerical method

High order (HO) method:

Problem

Let S_h be a collection of elements K, that partition the domain Ω. Let $V^h = \{u : \Omega \to \mathbb{R} \ : \ u \in C^0(\Omega), u|_K \in P^1(K), K \in S_h\}$. Let $\mathbf{u}_h = \sum_j U_j \phi_j$. Given $\mathbf{u}_h(\cdot, 0) = \mathbf{u}_0(\cdot) \in (L^2(\Omega))^m$, find $\mathbf{u}_h(\cdot, t) \in (V^h)^m$ a.e $(0, T]$ such that

$$\int_\Omega \phi \frac{\partial \mathbf{u}_h}{\partial t} dx + \int_{\partial\Omega} \phi \mathbf{f}(\mathbf{u}_h) \cdot \boldsymbol{n} d\sigma - \int_\Omega \nabla \phi \cdot \mathbf{f}(\mathbf{u}_h) d\boldsymbol{x} = \mathbf{0},$$

for all $\phi \in V^h$.

In matrix form, we solve for $\boldsymbol{U} = \{U_i\}$, where U_i is an approximation to $\mathbf{u}(\boldsymbol{x}_i)$:

$$\mathbf{M}_C \frac{d\boldsymbol{U}}{dt} + \boldsymbol{K}(\boldsymbol{U}) + \boldsymbol{B}_\Gamma(\boldsymbol{U}) = \mathbf{0}, \ t \in (0, T],$$

where

$$\mathbf{M}_C = \{M_{ij}\}_{i,j=1}^{N_h}, \ M_{ij} = m_{ij} I_{m\times m}, \ m_{ij} = \sum_e m_{ij}^{(e)}, \ m_{ij}^{(e)} = \int_{K_e} \phi_i \phi_j d\boldsymbol{x},$$

$$\boldsymbol{K}(\boldsymbol{U}) = \left\{ \sum_e - \int_{K_e} \nabla \phi_i \cdot \mathbf{f}(\mathbf{u}_h) d\boldsymbol{x} \right\}_i, \ \boldsymbol{B}_\Gamma(\boldsymbol{U}) = \left\{ \sum_e \int_{\Gamma\cap\partial K_e} \phi_i \mathbf{f}(\mathbf{u}_h) \cdot \boldsymbol{n} d\sigma \right\}_i.$$

Numerical method

Example

Burgers symmetric expansion:
$\Omega = (0, 4)$, $T = 1$. The conserved variable $\mathbf{u} = u$, $m = 1$. The flux is given by

$$\mathbf{f}(u) = \frac{1}{2}u^2\mathbf{v}, \ \ \mathbf{v} = \begin{cases} -1, & x \in (0,2), \\ 1, & x \in (2,4). \end{cases}$$

Discretize the HO scheme using Crank-Nicolson with $\Delta x = 4/200$, $\Delta t = 0.001$:

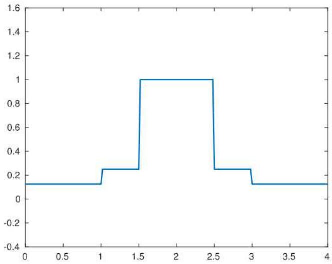

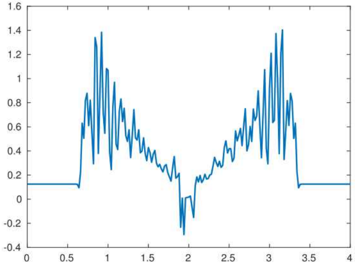

Numerical method

To *fix* the problem, we add some diffusion following the AFC design philosophy.

Low order (LO) method:

$$\mathbf{M}_L \frac{d\boldsymbol{U}}{dt} + \boldsymbol{K}(\boldsymbol{U}) + \boldsymbol{B}_\Gamma(\boldsymbol{U}) + \mathbf{D}(\boldsymbol{U})\boldsymbol{U} = \mathbf{0},$$

$$\mathbf{M}_L^{(e)} = \mathrm{diag}\{m_i^{(e)} I_{m\times m}\}_i, \text{ where } m_i^{(e)} = \sum_j m_{ij}^{(e)},$$

$$\mathbf{D} = \sum_e \mathbf{D}^{(e)}, \ \mathbf{D}^{(e)} = \{D_{ij}^{(e)}\}_{i,j}, \ D_{ii}^{(e)} = -\sum_{j\neq i} D_{ij}^{(e)}.$$

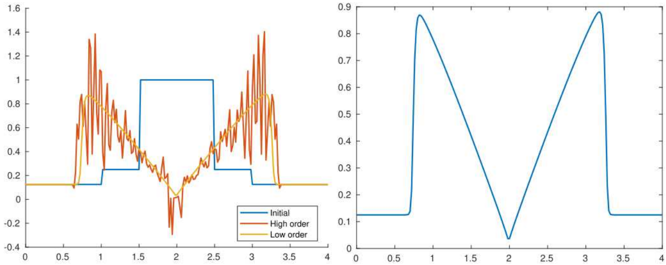

Artificial diffusion

Design based on the maximum propagation speed of the system.

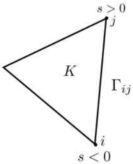

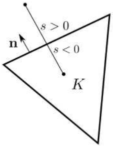

Consider a projected Riemann problem (Guermond et al. 2015, Selmin et al. 1996):

$$\mathbf{u}_t + \frac{\partial(\mathbf{f}(\mathbf{u}) \cdot \boldsymbol{n})}{\partial s} = \mathbf{0},$$

$$\mathbf{u}(\boldsymbol{x}(s), 0) = \begin{cases} \mathbf{u}_L, & s > 0, \\ \mathbf{u}_R, & s < 0. \end{cases}$$

Artificial diffusion

The maximum propagation speed for the above problem is denoted by

$$\lambda_{\max} = \lambda_{\max}(\boldsymbol{n}, \mathbf{u}_L, \mathbf{u}_R).$$

- The maximum propagation speed is such that $\mathbf{u}(s,t) = \mathbf{u}_R$ whenever $s/t \geq \lambda_{\max}$ and $\mathbf{u}(s,t) = \mathbf{u}_L$ for all $s/t \leq -\lambda_{\max}$.
- The max propagation speed is bounded above by the Lipschitz constant for $\mathbf{f} \cdot \boldsymbol{n}$.
- It is determined by the spectral radius of $\boldsymbol{n} \cdot \mathbf{f}'$.
- For nonlinear scalar problems, it is $\lambda_{\max}(\boldsymbol{n}, \mathbf{u}_L, \mathbf{u}_R) = \max(|\boldsymbol{n} \cdot \mathbf{f}'(\mathbf{u}_L)|, |\boldsymbol{n} \cdot \mathbf{f}'(\mathbf{u}_R)|)$.
- In finite elements $\mathbf{u}_{L,R}$ represent nodal states i and j, where $i \neq j$.

Artificial diffusion is constructed for the finite element formulation:

$$\mathbf{D}^{(e)} = \{D_{ij}^{(e)}\}_{i,j}, \; D_{ij}^{(e)} = d_{ij}^{(e)} I_{m \times m},$$

$$d_{ij}^{(e)} = \max\left\{\|\boldsymbol{c}_{ji}^{(e)}\|\lambda_{\max}(\boldsymbol{U}_i, \boldsymbol{n}_{ji}^{(e)}), \|\boldsymbol{c}_{ij}^{(e)}\|\lambda_{\max}(\boldsymbol{U}_j, \boldsymbol{n}_{ij}^{(e)})\right\}, \; j \neq i,$$

$$d_{ii}^{(e)} = -\sum_{j \neq i} d_{ij}^{(e)}, \; \boldsymbol{n}_{ij}^{(e)} = \frac{\boldsymbol{c}_{ij}^{(e)}}{\|\boldsymbol{c}_{ij}^{(e)}\|}, \; \boldsymbol{c}_{ij}^{(e)} = \int_{K_e} \nabla\phi_i \phi_j d\boldsymbol{x}, \text{ for each } K_e \in S_h.$$

Limiting algorithm

Pros of artificial diffusion and mass lumping:

- eliminates the spurious oscillations.
- makes the (nonlinear) problem easier to solve.

Drawback of artificial diffusion and mass lumping:

- Diffusion smears the profile
- Diminished accuracy

Solution to this problem:

- *Limiting* that controls the amount of diffusion introduced.
- Limiting that preserves the quality of the solution as possible.

Limiter for a quantity $u_h = \sum_j \phi_j u_j$:

$$\alpha_e^u = \min_{i \in N_h(K_e)} \Phi_i^u.$$

$\Phi_i^u \in [0,1]$ for $i = 1, ..., N_h$, satisfies the following conditions:

- $\Phi_i^u(u_i - u_j)$ depends continuously on u_j, $j \in N_i$.
- $\Phi_i^u(u_i - u_j) = 0$ at a local maximum and local minimum.
- $\Phi_i^u(u_i - u_j) = (u_i - u_j)$ if u_h is linear on Ω_i.

Limiter form on unstructured meshes for u (Kuzmin et al. 2018):

$$\Phi_i^u = 1 - \left[\frac{\left| \sum_{j\neq i} \beta_{ij}(u_j - u_i) \right| + \epsilon}{\sum_{j\neq i} \beta_{ij}|u_j - u_i| + \epsilon} \right]^q, \ \epsilon \approx 10^{-16}, q \geq 1,$$

where $\beta_{ij} > 0$ such that $\sum_{j\neq i} \beta_{ij} \boldsymbol{g}_i \cdot (\boldsymbol{x}_j - \boldsymbol{x}_i) = 0$.

$$\alpha_e^u = \min_{i \in N_h(K_e)} \Phi_i^u.$$

The final stabilized scheme

$$\mathbf{M}_L \frac{d\boldsymbol{U}}{dt} + \boldsymbol{K}(\boldsymbol{U}) + \boldsymbol{B}_\Gamma(\boldsymbol{U}) + \mathbf{D}(\boldsymbol{U})\boldsymbol{U} - \bar{\boldsymbol{F}}(\boldsymbol{U}) = \mathbf{0},$$

where

$$\bar{\boldsymbol{F}}(\boldsymbol{U}) = \sum_e \bar{\boldsymbol{F}}^{(e)}(\boldsymbol{U}),$$

is assembled from

$$\bar{\boldsymbol{F}}^{(e)}(\boldsymbol{U}) = \alpha_e^u \left[(\mathbf{M}_L^{(e)} - \mathbf{M}_C^{(e)}) \frac{d\boldsymbol{U}}{dt} + \mathbf{D}^{(e)}(\boldsymbol{U})\boldsymbol{U} \right].$$

Limiting algorithm

With limiting, the Burgers symmetric expansion has a steepened profile:

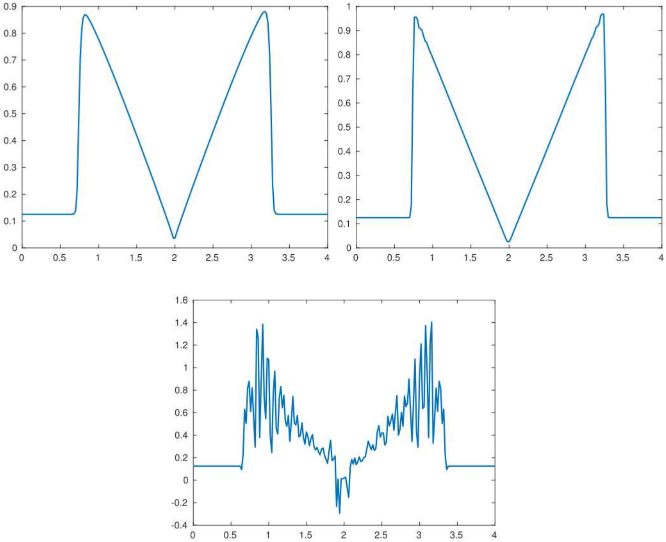

Recall that the Euler system has form

$$\frac{\partial \mathbf{u}}{\partial t} + \nabla \cdot \mathbf{f}(\mathbf{u}) = \mathbf{0},$$

where

$$\mathbf{u} = \begin{bmatrix} \rho \\ \rho \boldsymbol{v} \\ \rho E \end{bmatrix}, \ \mathbf{f}(\mathbf{u}) = \begin{bmatrix} \rho \boldsymbol{v} \\ \rho \boldsymbol{v} \otimes \boldsymbol{v} + pI \\ \rho E \boldsymbol{v} + p \boldsymbol{v} \end{bmatrix}.$$

The maximum propagation speed is computed from

$$\lambda_{\text{max}}(\mathbf{u}; \boldsymbol{n}) = \boldsymbol{v} \cdot \boldsymbol{n} + c,$$

where

$$c = \sqrt{\frac{\gamma p}{\rho}}$$

is the speed of sound.

Limiting procedure for Euler:

- **Synchronized limiting**: based on taking a minimum of several element limiters. For example,

$$\boldsymbol{\alpha}_e = \min\{\alpha_e^{\rho}, \alpha_e^{p}, \alpha_e^{\rho E}\} I_{m\times m}.$$

- **Segregated limiting**: limiting each sub-equation using a different limiter. For example,

$$\boldsymbol{\alpha}_e = \operatorname{diag}\{\alpha_e^{\rho}, \alpha_e^{\rho p}, \alpha_e^{\rho p}, \alpha_e^{\rho p}, \alpha_e^{\rho E}\}.$$

Then,

$$\bar{\boldsymbol{F}}(\boldsymbol{U}) = \sum_e \bar{\boldsymbol{F}}^{(e)}(\boldsymbol{U}),$$

where

$$\bar{\boldsymbol{F}}^{(e)}(\boldsymbol{U}) = \boldsymbol{\alpha}_e \left[(\mathbf{M}_L^{(e)} - \mathbf{M}_C^{(e)}) \frac{d\boldsymbol{U}}{dt} + \mathbf{D}^{(e)}(\boldsymbol{U})\boldsymbol{U} \right].$$

Transient HD results

Problems solved: Sod shocktube, Woodward-Colella blast wave, Sedov point blast etc... (Mabuza, Shadid and Kuzmin, 2018, JCP)

1D results; Top: Sod shock tube, Bottom: Woodward-Colella

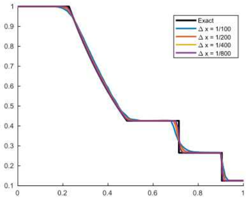

ρ vs x

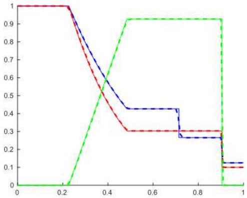

primitive variables vs x, for $\Delta x = \frac{1}{800}$

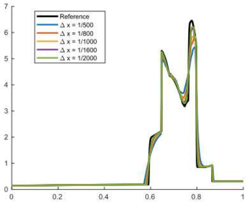

ρ vs x

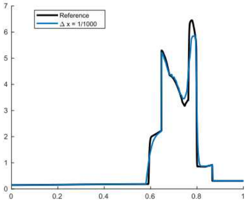

ρ vs x at $\Delta x = \frac{1}{1000}$

Sod ShockTube – Mesh Convergence 100-3200 cells

	L1 Slope (100-200)	L1 Slope (200-400)	L1 Slope (400-800)	L1 Slope (800-1600)	L1 Slope (1600-3200)
rho	9.36689e-01	9.65261e-01	8.52469e-01	8.06609e-01	8.60413e-01
rhoE	1.03158e+00	1.06352e+00	9.39890e-01	8.16929e-01	1.01285e+00
rhou	9.87064e-01	9.94115e-01	8.30446e-01	7.41841e-01	8.76973e-01

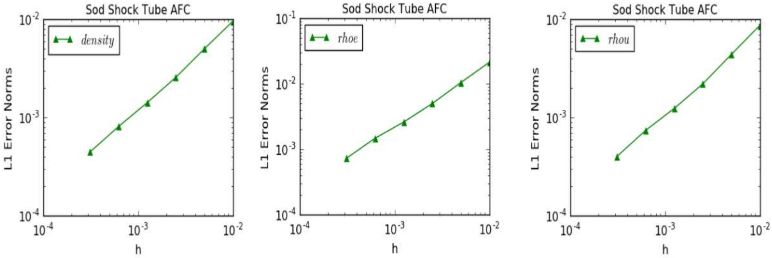

Transient HD results

LeBlanc ShockTube Profiles – Conservative CFD Formulation

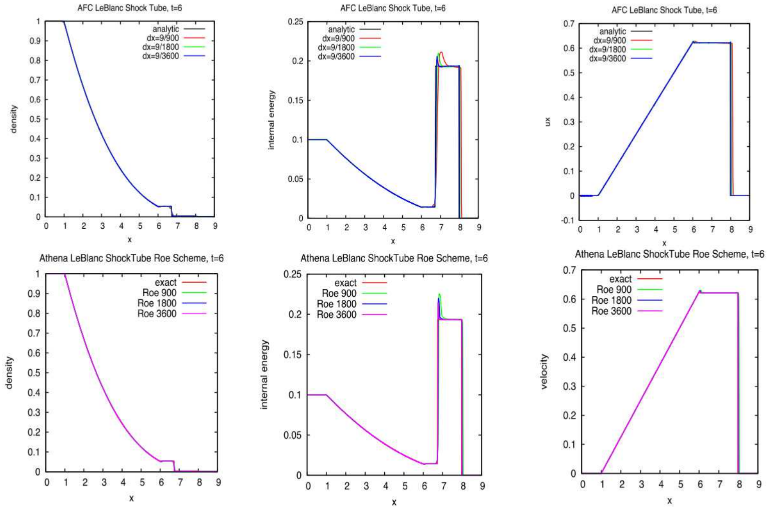

LeBlanc ShockTube – Mesh Convergence

	L1 error (9/900)	L1 error (9/1800)	L1 error (9/3600)	Slope (900-1800)	Slope (1800-3600)
rho	1.31065e-03	6.72218e-04	3.48644e-04	9.63279e-01	9.47172e-01
rhou	4.98398e-04	2.60317e-04	1.38587e-04	9.37030e-01	9.09481e-01
rhoE	1.91591e-04	9.83755e-05	5.14695e-05	9.61657e-01	9.34582e-01

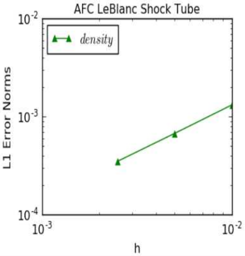

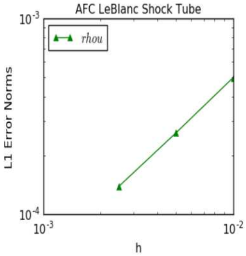

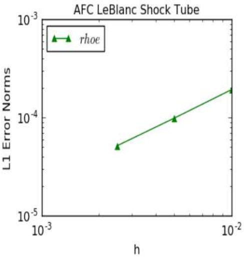

2D results; Top: Radial Riemann, Bottom: Sedov point blast

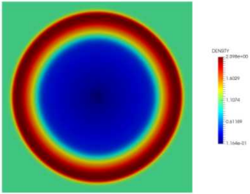

$\Delta x = \Delta y = 1/128$ and $\Delta t = 1 \times 10^{-3}$

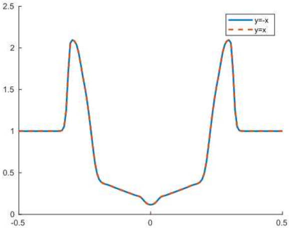

ρ vs x trace at $x = y$ and $y = -x$

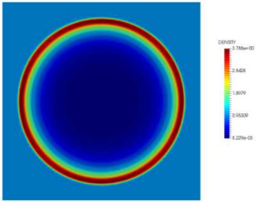

$\Delta x = \Delta y = 0.0125$ and $\Delta t = 1 \times 10^{-5}$.

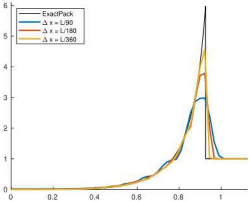

ρ vs x, $L = 2.25$ and $t = 0.24$.

Steady HD result

Steady $Ma = 3$ supersonic combustion ramjet engine:

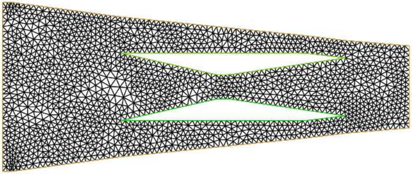

Coarse unstructured mesh

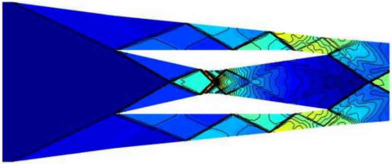

Density

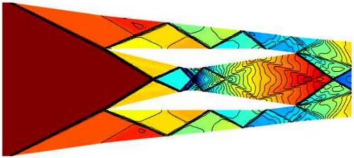

Mach

65256 elements and 33859 degrees of freedom per variable.

AFC for MHD

AFC for MHD with parabolic divergence cleaning:
The induction equation is given by (Dedner 2002)

$$\frac{\partial \boldsymbol{B}}{\partial t} + \nabla \cdot [\boldsymbol{v} \otimes \boldsymbol{B} - \boldsymbol{B} \otimes \boldsymbol{v}] - \nabla \cdot (c_p^2 \nabla \cdot \boldsymbol{B} I_{d\times d}) = \mathbf{0}.$$

MHD system has form

$$\frac{\partial \mathbf{u}}{\partial t} + \nabla \cdot \mathbf{f}(\mathbf{u}) + \nabla \cdot \mathbf{h}(\mathbf{u}) = \mathbf{0},$$

where
$\mathbf{h}(\mathbf{u}) = [0, \mathbf{0}, 0, -c_p^2 \nabla \cdot \boldsymbol{B} I_{d\times d}]$.
The maximum propagation speed is computed from

$$\lambda_{\max}(\mathbf{u}; \boldsymbol{n}) = \boldsymbol{v} \cdot \boldsymbol{n} + c_f.$$

At the semi-discrete level

$$c_p = \sqrt{c_h c_r}, \text{ where } c_r = 0.3,$$

where,

$$c_h = \max_e \left\{ \max_{j \neq i} \left[\|\boldsymbol{c}_{ij}^{(e)}\| \lambda_{\max}(\boldsymbol{U}_j; \boldsymbol{n}_{ij}^{(e)}) \right] \right\}, \ \boldsymbol{n}_{ij}^{(e)} = \frac{\boldsymbol{c}_{ij}^{(e)}}{\|\boldsymbol{c}_{ij}^{(e)}\|},$$

Limiting procedure for MHD:

- **Synchronized limiting**: based on taking a minimum of several element limiters. For example,

$$\boldsymbol{\alpha}_e = \min\{\alpha_e^{\rho}, \alpha_e^{p}, \alpha_e^{\rho E}\} I_{m\times m}.$$

- **Segregated limiting**: limiting each sub-equation using a different limiter. For example,

$$\boldsymbol{\alpha}_e = \mathrm{diag}\{\alpha_e^{\rho}, \alpha_e^{\rho e}, \alpha_e^{\rho e}, \alpha_e^{\rho e}, \alpha_e^{\rho E}, \alpha_e^{\frac{1}{2}\|\boldsymbol{B}\|^2}, \alpha_e^{\frac{1}{2}\|\boldsymbol{B}\|^2}, \alpha_e^{\frac{1}{2}\|\boldsymbol{B}\|^2}\}.$$

Then,

$$\bar{\boldsymbol{F}}(\boldsymbol{U}) = \sum_e \bar{\boldsymbol{F}}^{(e)}(\boldsymbol{U}),$$

where

$$\bar{\boldsymbol{F}}^{(e)}(\boldsymbol{U}) = \boldsymbol{\alpha}_e \left[(\mathbf{M}_L^{(e)} - \mathbf{M}_C^{(e)}) \frac{d\boldsymbol{U}}{dt} + \mathbf{D}^{(e)}(\boldsymbol{U})\boldsymbol{U} \right].$$

1D MHD test

Example (Brio-Wu test)

$\Omega = (0,1)$, $T = 0.1$, $B_x = 0.75$ and $\gamma = 2$, explicit RK4,
$(\rho, v_x, v_y, v_z, p, B_y, B_z)^L = (1, 0, 0, 0, 1, 1, 0)$,
$(\rho, v_x, v_y, v_z, p, B_y, B_z)^R = (0.125, 0, 0, 0, 0.1, -1, 0)$.

$\Delta x = \frac{1}{800}$, $\Delta t = 2.5 \times 10^{-4}$ Different synchronized limiting combinations vs Athena:

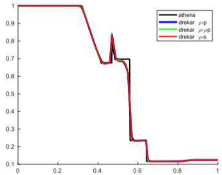

ρ vs x

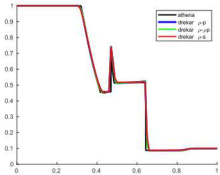

p vs x

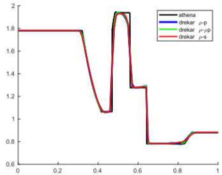

ρE vs x

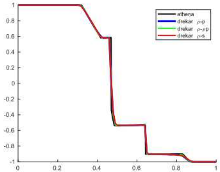

B_y vs x

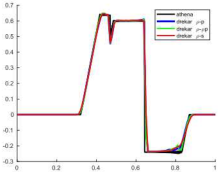

v_x vs x

1D MHD test

Example (Brio-Wu test)

$\Omega = (0,1)$, $T = 0.1$, $B_x = 0.75$ and $\gamma = 2$, explicit RK4,
$(\rho, v_x, v_y, v_z, p, B_y, B_z)^L = (1, 0, 0, 0, 1, 1, 0)$,
$(\rho, v_x, v_y, v_z, p, B_y, B_z)^R = (0.125, 0, 0, 0, 0.1, -1, 0)$.

Synchronized $\rho, \rho p$ limiting on various meshes:

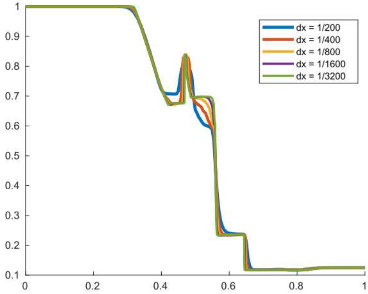

(a) density

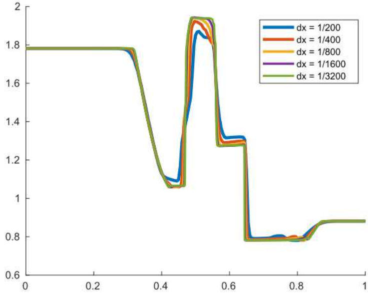

(b) total energy

1D MHD test

Example (Ryu-Jones test)

$\Omega = (-1, 1)$, $T = 0.2$, $B_x = \frac{2}{\sqrt{4\pi}}$ and $\gamma = \frac{5}{3}$, explicit RK4,

$$(\rho, v_x, v_y, v_z, p, B_y, B_z)^L = (1.08, 1.2, 0.01, 0.5, 0.95, \frac{3.6}{\sqrt{4\pi}}, \frac{2}{\sqrt{4\pi}}),$$

$$(\rho, v_x, v_y, v_z, p, B_y, B_z)^L = (1, 0, 0, 0, 1, \frac{4}{\sqrt{4\pi}}, \frac{2}{\sqrt{4\pi}}).$$

Synchronized $\rho, \rho p$ limiting on various meshes:

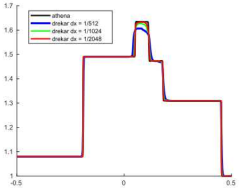

ρ vs x

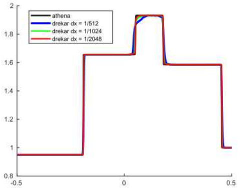

p vs x

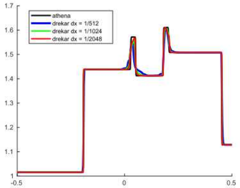

B_y vs x

2D MHD test

Example (Orszag-Tang)

$\Omega = (0,1) \times (0,1)$, $T = 0.2$, $B_x = \frac{2}{\sqrt{4\pi}}$ and $\gamma = \frac{5}{3}$, Crank-Nicolson + div. cleaning,

$$(\rho, v_x, v_y, v_z, p) = \left(\frac{25}{36\pi}, -\sin(2\pi y), \sin(2\pi x), 0, \frac{5}{12\pi} \right),$$

$$(B_x, B_y, B_z) = \left(-\frac{\sin(2\pi y)}{\sqrt{4\pi}}, \frac{\sin(4\pi x)}{\sqrt{4\pi}}, 0 \right).$$

Synchronized $\rho, \rho p$ limiting, $\Delta x = \Delta y = 1/256$, $\Delta t = 10^{-4}$

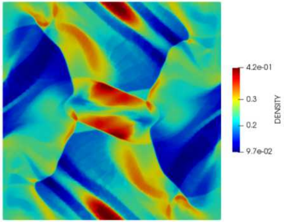

(a) no cleaning

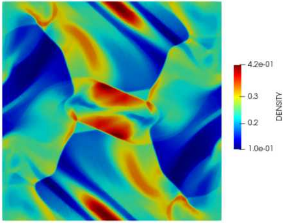

(b) parabolic cleaning

2D MHD test

Example (Orszag-Tang)

$\Omega = (0,1) \times (0,1)$, $T = 0.2$, $B_x = \frac{2}{\sqrt{4\pi}}$ and $\gamma = \frac{5}{3}$, Crank-Nicolson + div. cleaning,

$$(\rho, v_x, v_y, v_z, p) = \left(\frac{25}{36\pi}, -\sin(2\pi y), \sin(2\pi x), 0, \frac{5}{12\pi} \right),$$

$$(B_x, B_y, B_z) = \left(-\frac{\sin(2\pi y)}{\sqrt{4\pi}}, \frac{\sin(4\pi x)}{\sqrt{4\pi}}, 0 \right).$$

Synchronized $\rho, \rho p$ limiting, $\Delta x = \Delta y = 1/256$, $\Delta t = 10^{-4}$

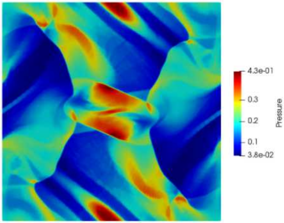

(a) no cleaning

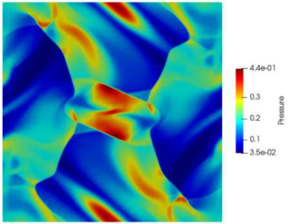

(b) parabolic cleaning

2D MHD test

Example (Orszag-Tang)

$\Omega = (0,1)\times(0,1)$, $T = 0.2$, $B_x = \frac{2}{\sqrt{4\pi}}$ and $\gamma = \frac{5}{3}$, Crank-Nicolson + div. cleaning,

$$(\rho, v_x, v_y, v_z, p) = \left(\frac{25}{36\pi}, -\sin(2\pi y), \sin(2\pi x), 0, \frac{5}{12\pi}\right),$$

$$(B_x, B_y, B_z) = \left(-\frac{\sin(2\pi y)}{\sqrt{4\pi}}, \frac{\sin(4\pi x)}{\sqrt{4\pi}}, 0\right).$$

Synchronized $\rho, \rho p$ limiting, $\Delta x = \Delta y = 1/256$, $\Delta t = 10^{-4}$; $\|\nabla \cdot \boldsymbol{B}\|_{L^2(\Omega)}$ vs t:

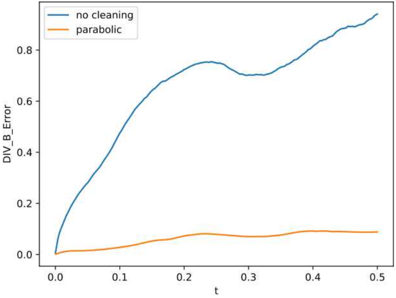

Incomplete bibliography

- D. Kuzmin, M. Möller, and M. Gurris, Algebraic Flux Correction II, Flux-Corrected Transport: Principles, Algorithms, and Applications, 2012, pp. 193–238.
- D. Kuzmin and J.N. Shadid, Gradient-based nodal limiters for artificial diffusion operators in finite element schemes for transport equations, International Journal for Numerical Methods in Fluids 84 (2017), no. 11, 675–695. fld.4365
- D. Kuzmin and S. Basting and J.N. Shadid, Linearity-preserving monotone local projection stabilization schemes for continuous finite ele- ments, Computer Methods in Applied Mechanics and Engineering 322 (2017), 23 –41.
- F. Fambri and M. Dumbser and O. Zanotti, Space-time adaptive ADER-DG scheme for dissipative flows: Compressible Navier-Stokes and resistive MHD equations, Computer Physics Communications 220 (2017), 297–318.
- S. Mabuza and J.N. Shadid and D. Kuzmin, Local bounds preserving stabilization for continuous Galerkin discretization of hyperbolic systems, Journal of Computational Physics (2018)
- M. Basting and D. Kuzmin, An FCT finite element scheme for ideal MHD equations in 1D and 2D, Journal of Computational Physics 338 (2017), 585–605.
- J-L. Guermond and B. Popov, Invariant domains and first-order continuous finite element approximation for hyperbolic systems, SINAM. vol 54, issue 4 (2016).